THE ASTROPHYSICAL JOURNAL, 421:542–549, 1994 February 1

SPECTROSCOPY OF CHROMOSPHERIC LINES OF GIANTS IN THE GLOBULAR CLUSTER NGC 6752[1]

A. K. DUPREE[2] AND LEE HARTMANN[2]
Harvard-Smithsonian Center for Astrophysics, 60 Garden Street, Cambridge, MA 02138
GRAEME H. SMITH[2]
University of California, Lick Observatory, Santa Cruz, CA 95064
A. W. RODGERS[2] AND W. H. ROBERTS
Mount Stromlo and Siding Spring Observatories, Private Bag, Weston Creek P.O., 2611, Canberra, ACT Australia
AND
D. B. ZUCKER
Harvard-Smithsonian Center for Astrophysics, 60 Garden Street, Cambridge, MA 02138
Received 1993 May 18; accepted 1993 August 9

ABSTRACT

Spectroscopic observations of chromospheric transitions (Mg II, Hα, and Ca II *K*) from two red giants (A31 and A59) in the globular cluster NGC 6572 were made with the Goddard High Resolution Spectrograph on the *Hubble Space Telescope* and the coudé spectrograph of the 1.9 m telescope at the Mount Stromlo Observatory. These measurements give evidence for chromospheric activity and outward motions within the atmospheres. The surface flux of the Mg II emission is comparable to that in disk population giants of similar $(B-V)$ color. The Mg II profiles are asymmetric, which is most likely caused by absorption in an expanding stellar atmosphere and/or by possible interstellar features. Notches are found in the core of the Hα line of A59, which are similar to those found in Cepheids. This suggests that shocks are present in the atmosphere of A59 and indicates that hydrodynamic phenomena are influencing the level of chromospheric emission and producing upper atmospheric motions which may lead to mass loss.

Subject headings: globular clusters: individual (NGC 6752) — shock waves — stars: chromospheres — stars: giants — stars: mass loss — ultraviolet: stars

1. INTRODUCTION

The information provided by the chromospheric lines of red giants in globular clusters is relevant to several fundamental problems in stellar evolution. Strong chromospheric emission from cool stars on the main sequence is believed to result from magnetic dynamo activity, yet the presence of chromospheric emission in the halo population of globular cluster red giants (Dupree et al. 1990a) is puzzling because the magnetic dynamo should be weak among such evolved old stars (Pasquini et al. 1991; Simon 1992). One goal of this study is to determine the level of the chromospheric emission among such red giants, and to search for spectroscopic evidence of the cause of the associated chromospheric activity. For example, short timescale variability of the Hα emission in metal-deficient field giants and a few globular cluster giants (Cacciari & Freeman 1983) suggests that these stars may be pulsating (Smith & Dupree 1988) and that hydrodynamic processes are influencing the properties of their chromospheres.

Profile asymmetry among chromospheric lines can reveal mass motions, and in particular the presence of mass loss in a stellar wind. Mass loss from red giants in globular clusters is demanded by stellar evolution theory to explain the spread in color of the horizontal branch stars (see, for instance, VandenBerg 1988 and Iben 1991), and to match the maximum luminosity of stars at the tip of the asymptotic giant branch (see Iben & Renzini 1983). Yet neither unambiguous spectroscopic signatures of mass loss from individual cluster red giants (excepting Mira-like variables, Frogel & Elias 1988), nor the resulting interstellar material assumed to collect in the cluster, have been detected (Roberts 1988; Faulkner & Smith 1991).

Profiles of chromospheric lines have the potential to reveal the signature of a stellar wind and circumstellar material, and several investigations utilizing this approach have been reported in the literature. Red giants in globular clusters exhibit rather low velocity shifts in the cores of the Hα or Na D lines (cf. Peterson 1981; Bates, Catney, & Keenan 1990; Bates, Kemp, & Montgomery 1993); these velocities are much less than the stellar surface escape velocities which amount to ≈ 60 km s^{-1}. Studies of metal-deficient field giants, which might be taken as surrogate stars for globular cluster giants, also indicate (slow) outflow as shown by asymmetries and line shifts in the Hα, Ca II, and Mg II lines (Smith, Dupree, & Churchill 1992; Smith & Dupree 1988; Dupree, Hartmann, & Smith 1990b). Most recently, the He I (λ10830) transition in one metal-deficient field giant was observed (Dupree, Sasselov, & Lester 1992) to show asymmetry associated with a fast wind, with speeds sufficient to escape the star. This marks a clear demonstration of true mass loss in an old thick-disk population giant. It is not known whether such speeds are prevalent among giants in globular clusters.

In this paper, we report the results of visible and ultraviolet spectroscopy of two of the brightest red giants in the globular cluster NGC 6752 to evaluate chromospheric flux levels and to search for evidence of the presence of stellar winds. Because the

[1] Based in part on observations with the NASA/ESA *Hubble Space Telescope* obtained at the Space Telescope Science Institute, which is operated by the Association of Universities for Research in Astronomy, Inc., under NASA contract NAS5-26555.

[2] Guest Observer, NASA/ESA *Hubble Space Telescope*.

interstellar reddening toward the cluster is extremely low, NGC 6752 offers an attractive target for ultraviolet measurements.

2. OBSERVATIONS AND DATA REDUCTION

The two target stars, A31 and A59 in NGC 6752 (Alcaino 1972), were observed in the chromospheric line of Mg II with the Goddard High Resolution Spectrograph (GHRS) on the *Hubble Space Telescope* (*HST*), and shortly thereafter in Hα and the Ca II K line at the Mount Stromlo Observatory. The physical characteristics of our target stars, together with references to the sources of these data, are summarized in Table 1. These stars were chosen for observations because they display Hα emission wings in their spectra (Cacciari & Freeman 1983) and Mg II emission had been detected in spectra taken with the *International Ultraviolet Explorer* (*IUE*) at low resolution (Dupree et al. 1990a). The positions of the stars used for pointing the *HST* were determined by scanning photographic plates of the cluster, and placing the measured coordinates in the reference frame of the *HST* Guide Star Catalog. The plate scanning and astrometric reductions were carried out at the Space Telescope Science Institute (STScI) using plates of NGC 6752 loaned from the Mount Stromlo Observatory archives.

2.1. *The GHRS Spectra of* Mg II

The target red giants are sufficiently faint at ultraviolet wavelengths to make them demanding targets for the *HST*/GHRS at moderate resolution. Fortunately, observations with *IUE* in the low-dispersion mode, which required ≈14 hr of integration (Dupree et al. 1990a), enabled us to estimate the expected flux levels for the GHRS measurements. Guest observer time on *HST* was awarded during cycle 1 for 9 hr of spacecraft time. The observations were initiated beginning 1992 April 16, and extended over 47 hr.[3] Four hours of total integration with the intermediate-resolution G270M grating were planned for each target, and this amount was acquired successfully.

The pointing for our targets was carried out during dark time with a blind acquisition using the Large Science Aperture (LSA) followed by a LOCATE command. Because the GHRS identifies targets based on ultraviolet flux and NGC 6752 has a population of hot horizontal branch stars which might inadvertently fall in the aperture, our red giants were not acquired with standard spiral search procedures. An ultraviolet map of the aperture (16 × 16 pixel map) using the focus diodes was taken during dark time to verify that our targets were indeed in the aperture. The *HST* pointing placed the stars within 0.″375 of the center of the LSA; maximum counts in the aperture map were 44 (A31) and 45 (A59) for a 7 s integration period. Because the 0.″375 offset within the LSA fortunately lay along the direction perpendicular to the dispersion (i.e. the y axis of the aperture), there was essentially no impact on the resolution or the wavlength scale of the resulting spectra. The data, processed with the standard pipeline processing procedures by the STScI, were delivered to the Center for Astrophysics with a polynomial background removed and with a vacuum wavelength calibration. We re-reduced the data using the pipeline programs of STSDAS, removed a constant background (now the usual procedure), and changed the wavelength scale to air.

The spectra were obtained in a standard mode of the GHRS in which the total exposure time is divided into four equal segments, each taken at a slightly different carousel setting so as to minimize the fixed pattern noise on the detector (dubbed an FP-SPLIT procedure). For our program, each of these segments was in turn composed of some 15 short subexposures, ≈3.8 minutes in duration, intended to reduce the effects of the spectrum drift resulting from the changing thermal and magnetic environment of *HST*. We could not use the customary procedure of cross correlating the individual 3.8 minute subexposures to remove the thermal drift and geomagnetically induced image motion because the signal-to-noise ratio in the individual subexposures is low. Instead, we obtained a time line of the commands and data transmissions from *HST* during execution of our program, and formed groups by selecting subexposures made at the same carousel setting that were sequential in time. These groups typically contained three to five subexposures and were separated by occultations and waits for target reacquisition. The typical separation between groups was 45 minutes to 3 hr with a minimum time of 30 minutes. The flux-calibrated subexposures in each group were averaged, and the resulting spectra for those groups which had been acquired at the same carousel setting were cross correlated with each other, aligned, and then averaged; the contribution of each group spectrum was weighted by the number of subexposures it contained. In this way, a spectrum was obtained for each of the four carousel settings in the sequence. These four spectra were then cross correlated to that for the last carousel position, and the wavelength scale corresponding to this last position was adopted. We hope to have minimized thermal deviations by using the last wavelength scale, since the telescope should have stabilized by the end of the observation.

TABLE 1

PARAMETERS OF TARGET STARS

Quantity	A31	A59	References
R.A. (2000.0)	$19^h11^m11^s.282$	$19^h10^m32^s.312$	1
Decl. (2000.0)	−59°59′53″.89	−59°57′06″.25	1
V	10.80	10.90	2
$B-V$	1.60	1.59	2
$E(B-V)$	0.03	0.03	3
$(V-R)_0$	1.23	1.20	4
ϕ[a]	0.255	0.233	
M_V	−2.8	−2.7	
$T_{\rm eff}$ (K)	3915/3950	3926/4050	3, 5
$M_{\rm bol}$	−3.52	−3.39	6
$R(R_\odot)$	97.4	91.2	
$RV_{\rm helio}$ (km s^{-1})	−26.1	−18.4	1
$F_{\rm obs}$:λ2795[b]	6.1E−15	3.4E−15	
$F_{\rm obs}$:λ2802[b]	7.1E−15	4.0E−15	
F_*:λ2795[c]	1.9E+4	1.3E+4	
F_*:λ2802[c]	2.2E+4	1.5E+4	

[a] Angular diameter in units of 10^{-3} arcsec; derived following Barnes, Evans, & Moffett 1978, and assuming $A_V = 3.3E(B-V)$.

[b] Units of ergs cm^{-2} s^{-1} observed at Earth in Mg h and k emission cores.

[c] Units of ergs cm^{-2} s^{-1} from stellar surface. $F_* = 1.702 \times 10^{17}/\phi^2$. F_* has been corrected for reddening where $A_{\lambda 2000} = 6.1E(B-V)$; Seaton 1979.

REFERENCES:—(1) This work; (2) Cannon & Stobie 1973; (3) Frogel et al. 1983; (4) Based on the $(V-R)_0$–$(V-K)_0$ relation given by Johnson 1966 and $(V-K)_0$ colors measured by Frogel et al. 1983; (5) Pilachowski, Sneden, & Wallerstein 1983; (6) Frogel, Persson, & Cohen 1981.

[3] The inefficient use of *HST* time can be attributed to two software problems: our request for a dark acquisition was misinterpreted as a request for spectra to be accumulated during dark time; and the software failed to recognize that our targets were in the continuous viewing zone of *HST*.

A spectrum was then formed from all of the data obtained for each star. A wavelength calibration exposure (SPY-BAL) was taken automatically at the end of each target pointing; the difference between the *HST* pipeline wavelength calibration and our fit to the platinum arc from the exposure at each target, was used to apply an offset of the standard wavelength calibration. The offset amounted to -0.03 Å (target A59) and -0.08 Å (target A31). Both of these offset values are comparable to or less than the expected wavelength uncertainty of ± 1 full diode width or ± 0.09 Å which equals ± 9 km s^{-1} (Duncan 1992). The final spectra are shown in Figure 1. The signal-to-noise ratio of these spectra is not sufficient to justify a deconvolution procedure.

In 1993 March, after our data were reduced, the STScI advised that in some cases the Doppler compensation procedure within the GHRS was applied incorrectly, leading to corruption of data taken at velocity extrema of the *HST* with respect to our targets. The maximum possible change between exposures amounts to 15.2 km s^{-1}. The Mg II emission lines are broad with typical base widths of ≈ 150 km s^{-1}, so that the maximum effects would be small as compared to the line base width.

Software (*obsum* within STSDAS) provided by the STScI demonstrated that 10% of our 4 minute exposures were "definitely" affected, with a maximum of 61 s per exposure spent at a velocity extremum without proper Doppler compensation. An additional 17% of the ≈ 60 exposures on each target was identified as "potentially affected." However, this latter number is most likely an overestimate because the STSDAS software simply flagged time intervals during which the spacecraft passed through velocity extrema, without verifying that our exposures were actually underway. A large number of such spurious intervals exist because our observing program made inefficient use of *HST* time as discussed above. Examination of individual 4 minute exposures to assess the presence of the Doppler compensation error was inconclusive because the signal-to-noise ratio in the individual exposures is too low to determine whether the wavelength is shifted or whether broadening of the Mg II line profiles occurs due to the time spent at uncorrected redshifts or blueshifts. If we omit all of the potentially corrupt exposures, and co-add the remaining spectra, the profiles that result show little difference from those that incorporate all of the data. Thus we used all of the data in our analysis.

The Mg II profiles (Fig. 1) are exceptionally asymmetric, indicating substantial absorption of the chromospheric emission on the short-wavelength side of the lines. The observed emissions have a width of 1.5 to 2.0 Å at the base of the line profile. Because the projection of the LSA (2 × 2 arcsec square) on the spectrum amounts to eight diodes (the scale is 0.″25 per diode) corresponding to ≈ 0.7 Å, we are confident that the spherical aberration of the *HST* is not responsible for the line asymmetry.

The flux observed in each emission line was derived by fitting a local continuum (to compensate for the residual background) and integrating the emission spectrum directly. The absolute calibration is provided by the STScI and is expected to have an accuracy of $\pm 10\%$ (Soderblom 1993). The values of these fluxes are listed in Table 1, as are several other derived properties of these stars.

Previous observations of the Mg II emission in these giants were made (Dupree et al. 1990a) using the low-dispersion mode of *IUE* in which the doublet was not resolved. The contribution of the local continuum could not be separated from the Mg II emission feature, hence lower and upper limits to the line flux were obtained that correspond to the removal or inclusion of a local continuum, respectively. For A31, the total GHRS fluxes for the doublet emission agree well with the observed fluxes derived from *IUE* low-dispersion spectra (Dupree et al. 1990a), lying between the lower and upper limits. However, the GHRS flux appears lower for A59, by a factor of 2.5, than the minimum estimated flux from the *IUE* spectrum. Consideration of the expected error limits on the fluxes measured with *IUE* (30%) and GHRS (10%) does not account for the differ-

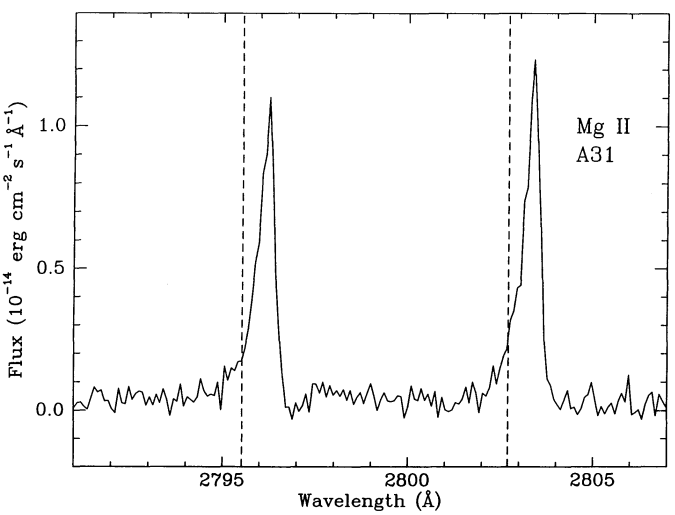

FIG. 1*a*

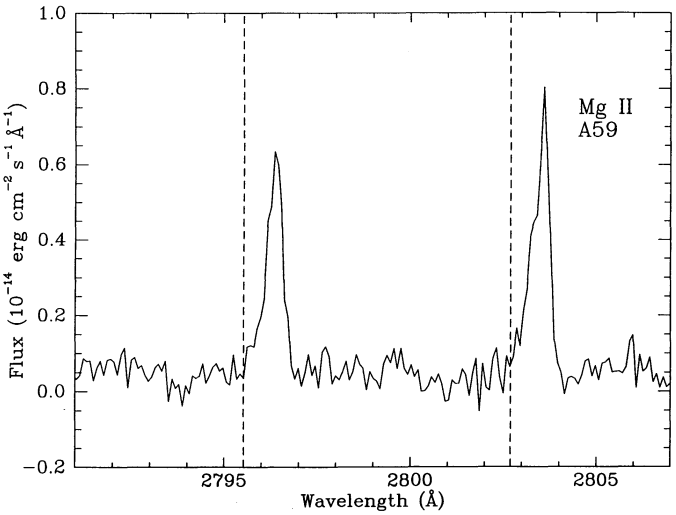

FIG. 1*b*

FIG. 1.—The GHRS spectra of the Mg II doublet [λ2795.523, λ2802.698 (air)] in two red giants, A31 and A59 in the globular cluster NGC 6752. The vacuum wavelength scale obtained from the GHRS has been converted to air, and by our measured heliocentric photospheric velocity for each star. Thus the plotted wavelength scale is given in the photospheric rest frame of each star. The vertical dashed lines mark the position of the expected central wavelength of the Mg doublet lines. The spectra are binned by 4 pixels (≈ 0.1 Å).

ence between the two observations of A59, indicating that the difference is real, and that the Mg II flux of A59 has varied between 1987 and 1992.

2.2. *The Optical Spectra*

The coudé spectrograph on the 1.9 m telescope at Mount Stromlo and Siding Spring Observatories (MSSSO) was used to obtain Hα and Ca II K spectra of our targets on the nights of 1992 May 5–9. The 32 inch (81 cm) focal length spectrograph camera was employed with a 600 line grating operating in fourth order for the K line and third order for Hα. The projected slit width equaled two detector pixels (2 × 15 μm) or 0".6 on the sky. The detector used was the MSSSO photon-counting array with a blue-sensitive S20 cathode (Rodgers et al. 1988). Exposures amounted to 20,000 s for the Ca K line and 3000 s for Hα. Wavelength calibration was achieved via thorium/argon arc lamp exposures. Reductions of the data were made at MSSSO using the NOAO/IRAF package.

The radial velocities of A31 and A59 were measured from the coudé spectra based on the observed wavelengths of photospheric metal lines near λ6440. The calibration of the thorium/argon comparison arc exposures resulted in a mean residual error of 0.008 Å averaged over the length of the spectra, and we estimate that the absolute values of the photospheric velocities are correct to ±3 km s^{-1} while the velocity of the chromospheric features, the Ca II K and Hα lines, relative to the photospheric lines are equally well established. The photospheric velocities are given in Table 1. The Hα and Ca II K spectra shown in Figure 2 are placed on a heliocentric velocity scale.

3. DISCUSSION

The chromospheric transitions can indicate mass flow in the atmospheres of stars, as well as the level of radiative losses that relates to the energy balance. We address each of these phenomena and also consider the presence of interstellar absorption through the low-latitude galactic halo which may modify the ultraviolet Mg II line profiles.

3.1. *The Optical Spectra:* Hα *and* Ca II (K)

The Hα and Ca II K profiles are typical of those found in the spectra of other relatively bright ($M_V \leq -1.7$) metal-deficient red giants both in globular clusters and in the field (see, for examples, the spectra of these lines shown in the papers of Cohen 1976; Peterson 1982; Smith & Dupree 1988; Smith et al. 1992). The Ca II K emission reversal is prominent and symmetric in both stars implying that little mass motion is present in the region of the atmosphere in which this feature forms at the time of the observations. The radial velocity of the reversal at the center of the emission features is −1 and −3 km s^{-1} relative to the photospheric lines for A31 and A59, respectively. These spectra give little indication of interstellar calcium along the line of sight. The stellar radial velocities are negative, and interstellar Ca II might contribute to a weakening of the long-wavelength side of the emission, but it is not strong if it is present at all, in view of the symmetry of the emission. The noise in our spectra does not allow interstellar features to be ruled out, however. The Ca II profile in A31 resembles our spectrum taken in 1986 (Dupree et al. 1990a), but the A59 profile had a strong long-wavelength emission wing in 1986 as compared to the 1992 profile.

The Hα profiles shown in Figure 2 are similar to our 1986 spectra in terms of their emission wings, although the present spectra show a modest strengthening of the long-wavelength emission in comparison to the short-wavelength emission. This is not surprising since the emission strength in A31 has been found to vary on a timescale of ≈3 weeks (Cacciari & Freeman 1983). The velocities of the Hα absorption cores relative to the photosphere correspond to −7.5 and −4 km s^{-1} for A31 and A59, respectively, values typical of metal-deficient field giants for stars of similar luminosity (Smith & Dupree 1988).

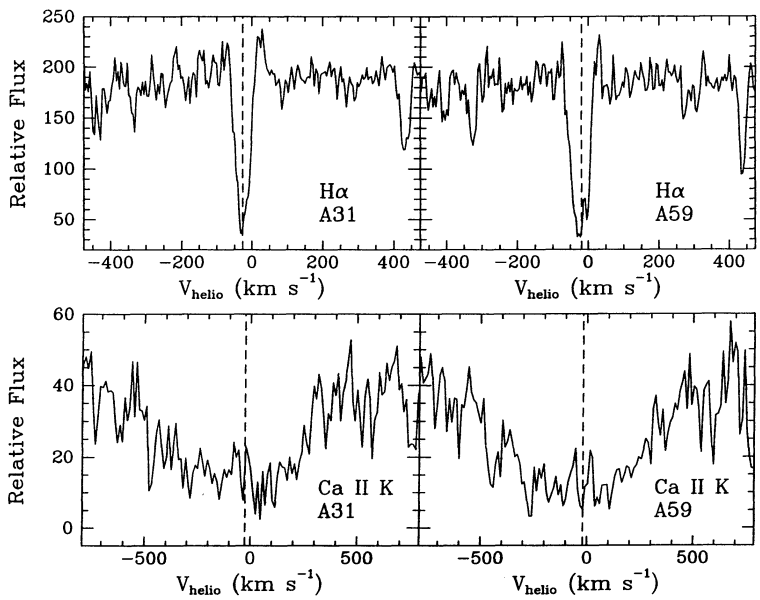

FIG. 2.—Echelle spectra of the Hα (λ6562.82) and Ca II K line (λ3933.66) profiles in A31 and A59 obtained at the 1.9 m telescope of Mount Stromlo Observatory. The dashed vertical line denotes the expected position of the stellar photospheric line centers. Note the signature of atmospheric expansion in the Hα core as indicated by the core asymmetry and shift to shorter wavelengths. The two features in the Hα core of A59 (at −7.5 and +15 km s^{-1} relative to the photosphere) are believed to indicate shock waves in the atmosphere since they resemble those observed and calculated in Cepheids. The Ca II K core reversals (K_3) display modest velocity shifts: −1 to −3 km s^{-1}.

Most significant may be the doubling of the Hα absorption core in the spectrum of A59. The two features in the core lie at -7.5 and $+15$ km s^{-1} with respect to the stellar photospheric velocity as defined by metal lines. Similar features occur in the Hα profiles at some phases of the classical Cepheids, *l* Carinae (Rodgers & Bell 1968), T Mon and X Cyg (Wallerstein 1972, 1983) and the Population II Cepheid κ Pav (Wallerstein et al. 1992), although the separation between the two core features is more substantial ($\approx$60 km s^{-1}) for the Cepheids than is found here (22.5 km s^{-1}). Early models of Cepheid atmospheres (Karp 1975) indicated the occurrence of line-splitting, and the more recent time-dependent codes with full radiative transfer considerations predict Hα profiles with cores that are split (Sasselov 1993), similar to our observations. In addition, the chromosphere of A59 varies in its structure as shown by the 1987 spectra which displayed outflow in the Ca II K line and a stronger Mg II emission flux than in the 1992 spectra. We take these measurements and the associated theoretical calculations as additional evidence for pulsation in the atmospheres of metal-poor red giants like A59.

The optical spectra suggest that differential outward mass flow is present in the chromospheres of A31 and A59; the lower expansion velocity of the Ca II K_3 reversal and the symmetry of the K_2 lines as compared to the higher expansion velocities found for the Hα core are consistent with steady state models of metal-deficient red giants with expanding atmospheres, since the calcium emission (K_2) is formed below the level of the Hα absorption core (Dupree, Hartmann, & Avrett 1984).

3.2. *The Ultraviolet* Mg II *Lines*

The stellar surface fluxes of the Mg II lines as derived from the spectra are comparable to those of giant and supergiant stars of Population I (see Fig. 3). In spite of substantial metal deficiencies in the globular cluster stars, the radiative losses from the Mg II lines do not reflect lower values that would result if they were simply scaled by the magnesium abundance. The observed surface fluxes are corrected for the ultraviolet extinction corresponding to $E(B-V) = 0.03$, but the values may still underestimate the true surface flux due to possible absorption from interstellar Mg II. These observations confirm the strong chromospheric emissions in the oldest evolved stars in our Galaxy, and reinforce the conclusion that magnetic chromospheric activity is not the principal contributor to these line strengths. Among red giants in an old stellar population, the magnetic dynamo would not function efficiently, if at all. The progenitor main-sequence stars, i.e., subdwarfs, represent the oldest dwarfs in the Galaxy, and according to the Skumanich (1972) relation (see also Simon, Herbig, & Boesgaard 1985), or considering their lowered rotation rates (Simon 1990), their dynamos and chromospheric activity might be expected to be relatively weak by comparison with Population I dwarfs. In addition, fluxes in chromospheric emission lines are observed to drop markedly in association with the evolution of a former dwarf into the subgiant region of the H-R diagram (Simon & Drake 1989).

The interpretation of the Mg II line profiles is not straightforward. A differentially expanding chromosphere would produce an asymmetric profile as is observed. In fact, the shape of the Mg II line profiles in our targets is very similar to that of the nearby, slightly metal-deficient giant, α Boo (see Fig. 4). However, A31 is intrinsically more luminous and cooler than α Boo [$(B-V)_0 = +1.3$; $M_V = -0.04$]. Thus A31 should have a much wider emission profile as judged by correlations based on the Wilson-Bappu effect (Weiler & Oegerle 1979). If the Mg II profiles are assumed to have the same extent to short wavelengths as toward long wavelengths, they should reach to -125 or -150 km s^{-1}, and in that case the predicted $M_V \approx -3$ (Weiler & Oegerle 1979) is in good agreement with the magnitudes determined from the distance modulus to the cluster (see Table 1). The possibility of a metallicity dependence on the absolute magnitude calibration has been addressed for only one metal-deficient star (Dupree et al. 1990b), and for that

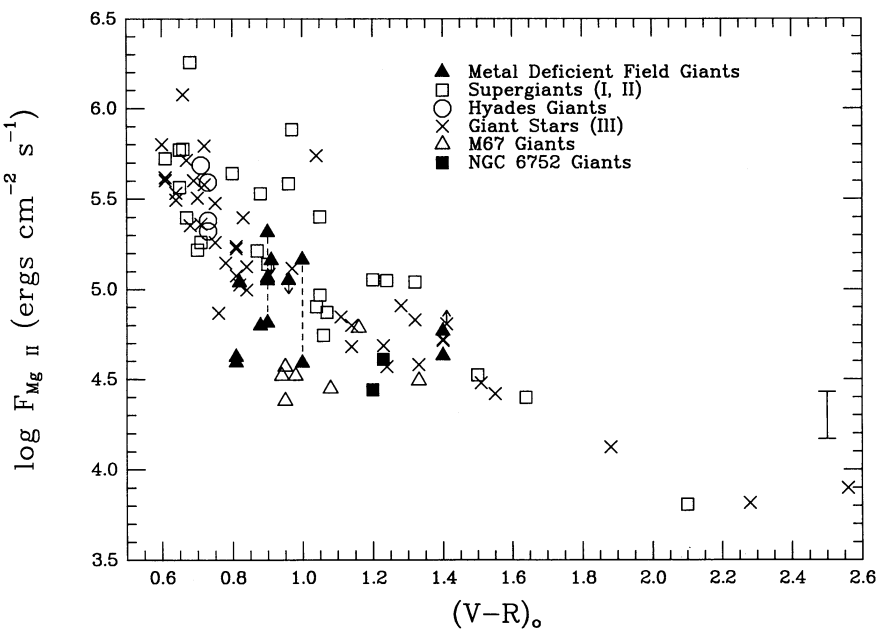

FIG. 3.—The stellar surface flux in Mg II of the giants in NGC 6752 as compared to other luminous stars. A tabulation of the comparison stars and their fluxes is contained in Dupree et al. (1990b).

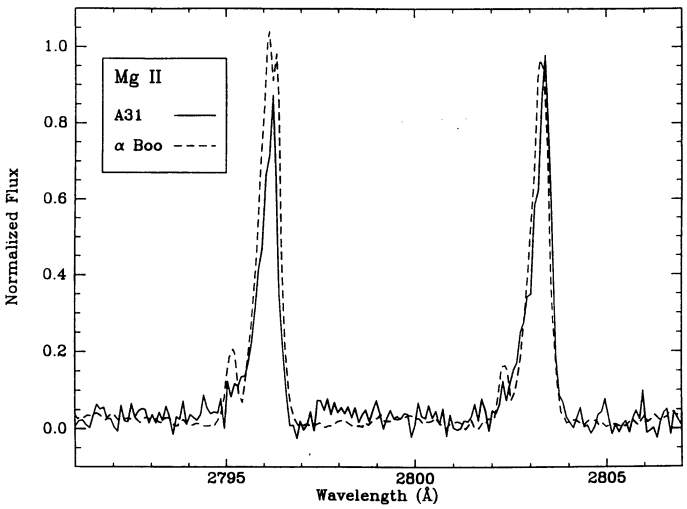

FIG. 4.—The Mg II doublet in A31 as compared to an *IUE* spectrum (LWR 4435) of α Boo obtained from the NSSDC. Although α Boo is less luminous and hotter than A31, and 10 pc distant (so the interstellar absorption is minimal), the similarity between the two profiles is striking. The signal-to-noise ratio in the wings of A31 is not high enough to identify possible narrow absorption features or weak emission.

object the Wilson-Bappu relation appeared to be satisfied provided that the appearance of the Mg II profile was modified by opacity in a stellar wind. The narrow profiles in A31 could be used to argue that the mass loss in this globular cluster giant is substantially higher than in α Boo, so that part of the short-wavelength side of the Mg II profile in A31 is absorbed by the stellar wind.

To assess the impact of interstellar Mg II absorption upon the observed profile, we summarize the characteristics of the interstellar medium in the direction of NGC 6752.

3.3. *The Line of Sight toward NGC 6752*

Our targets were chosen for *HST* observations because they are relatively bright for globular cluster stars, and lie in a cluster with low reddening at $l = 336\overset{\circ}{.}5$ and $b = -25\overset{\circ}{.}6$. However, the interstellar resonance lines of Mg II can be strong. Even low values of $E(B-V) \leq 0.05$ can be associated with equivalent widths of 0.6 to 0.7 Å in the Mg II doublet (deBoer et al. 1986); higher values can produce saturation in Mg II over 1.1 Å (120 km s^{-1}; cf. Sembach, Savage, & Massa 1991). Values of $E(B-V)$ for NGC 6752 range from 0.0 (Da Costa, Armandroff, & Norris 1992; Zinn 1980), 0.03 (Harris & Racine 1979), 0.04 (Cannon 1974), and 0.05 (Cannon & Stobie 1973). The distance modulus $(m-M)_V = 13.20$ (Harris & Racine 1979) which, for $E(B-V) = 0.03$, gives a distance of 4.2 kpc from the Sun and 1.8 kpc below the plane of the Galaxy. If the asymmetry in the Mg II lines were attributed completely to interstellar medium absorption, the inferred disk and halo material would be distributed in velocity from $V_{LSR} = -120$ to $+41$ km s^{-1} toward A31, with a similar large spread ($V_{LSR} = -65$ to $+70$ km s^{-1}) toward A59.[4]

There are three potential sources of interstellar absorption features:

i. A survey of H I emission (Colomb, Pöppel, & Heiles 1980) shows faint wisps of emission near $V_{LSR} = 0$ km s^{-1} toward NGC 6752 in photographic representation, but no features outside of these velocities. There are no high-resolution spectroscopic studies of interstellar absorption features, nor any high-velocity clouds toward the cluster (Wakker & van Woerden 1991).

ii. A very local interstellar component (Crutcher 1982), if present in the direction of NGC 6752, would appear in the spectrum at $V_{LSR} = -14.5$ km s^{-1}. Judging from Mg II profiles of nearby giants (Molaro, Vladilo, & Beckman 1986), such absorption would not obscure the short-wavelength wing of our line profiles.

iii. The velocity of the rotating Galactic disk material in the direction of NGC 6752 can be evaluated using disk rotation curves (Clemens 1985) for a solar galactocentric distance of 8.5 kpc, a solar neighborhood circular motion around the Galactic center of 220 km s^{-1}, and the assumption of corotation. The velocities become progressively more negative and reach $V_{LSR} \approx -50$ km s^{-1} at the 4.2 kpc distance of the cluster (Sembach 1993).

The positions of the three potential absorbers in the direction of NGC 6752 are shown in Figure 5 with respect to the stellar Mg II line profiles. The uncertainty in the zero point of the GHRS wavelength scale corresponds to ± 9 km s^{-1} (Duncan 1992), an amount insufficient to change the relative positions significantly. If interstellar Mg II were sufficiently abundant, it could be responsible for some of the observed line asymmetries. However, it does not appear likely that all of the absorption is attributable to interstellar Mg II because the observed profile shows neither the wing shape nor the optical depth found in interstellar line profiles. In A31, detectable stellar flux extends from $V_{LSR} = -75$ to $+50$ km s^{-1}, the positive value being associated with the peaks of the emission. Emission at negative velocities is not as extensive in the spectrum of A59, yet ranges from -10 to $+75$ km s^{-1} at its peak. Observed spectra of interstellar Mg II lines are optically thick in the cores and can absorb all flux over considerable velocity ranges. Moreover, the wings of the Mg II lines are typically sharp, falling from the continuum level to zero in the line core over ≈ 50 km s^{-1} (cf. Sembach et al. 1991; Danly et al. 1992). Both of these considerations suggest that the asymmetry in the Mg II profiles is not typical of a pure interstellar Mg II absorption profile.

3.4. *The Stellar Mass-Loss Rate*

If the interstellar Mg component was minimal, then the Mg II line asymmetries would result from a stellar wind that has a terminal velocity of ≈ 150 km s^{-1}. Such a speed exceeds both the stellar photospheric escape velocity (55 km s^{-1}) and the escape velocity from the cluster core (23 km s^{-1}, Webbink 1981). The presence of a fast wind would resolve the long-standing puzzle of the apparent lack of interstellar material in globular clusters (cf. Roberts 1988; Smith et al. 1990).

The mass-loss rate indicated by these profiles can be estimated if they are produced by a stellar wind. The Sobolev optical depth for a linear velocity law in a rapidly expanding atmosphere is (Castor 1970):

$$\tau_s \sim \frac{\pi e^2}{mc} \frac{\lambda_0 f N_{Mg} R}{V},$$

where the stellar radius, R, is taken as the characteristic length, λ_0 is the wavelength at line center, N_{Mg} is the Mg density, and

[4] In the direction of NGC 6752, the relation between the velocity reduced to the local standard of rest and the heliocentric velocity is given by $V_{LSR} = V_{helio} - 0.13$ km s^{-1}, assuming a solar speed of $+16.5$ km s^{-1} in the direction (epoch 1950.0) $l = 53°$, $b = 25°$ (Mihalas & Binney 1981).

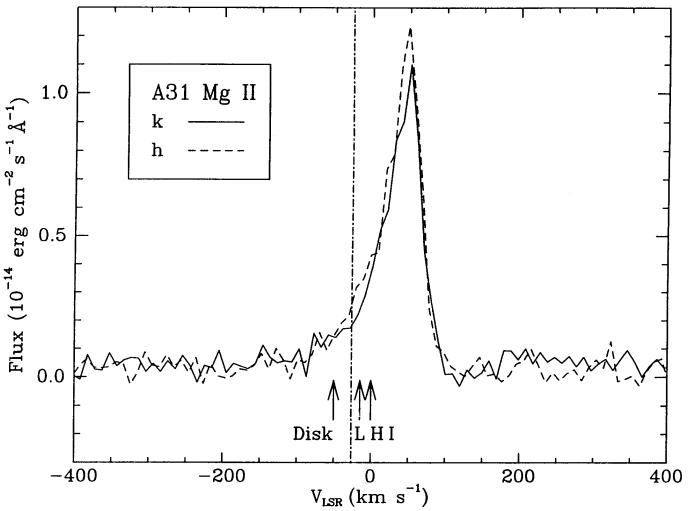

FIG. 5a

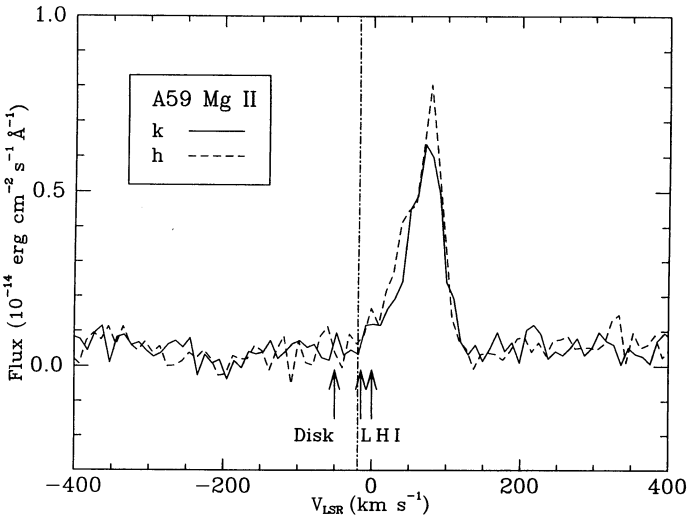

FIG. 5b

FIG. 5.—The $h(\lambda 2802)$ and $k(\lambda 2795)$ lines of Mg II in A31 and A59 superposed on a velocity scale referenced to the local standard of rest (LSR). The vertical broken lines mark the stellar photospheric velocity. Sources of possible interstellar Mg II absorption in the direction of NGC 6752 ($l = 336.5°$ and $b = -25.6°$) are indicated by arrows: the expected velocity of the local interstellar material (*L*) as determined by Crutcher (1982); the velocity of hydrogen observed in emission (H I) by Coulomb et al. (1980); and the maximum velocity extent for the rotation of the galactic disk (*Disk*) in the direction of, and at the distance (4.2 kpc) of NGC 6752.

V is the wind velocity. Substituting for N_{Mg} into the mass-loss rate, $\dot{M} = 4\pi R^2 N_H \mu_H V$, where $N_{Mg} = N_H A$, we find

$$\dot{M} \sim 0.7 \times 10^{-9} \tau_s \left(\frac{R}{100 R_\odot}\right)\left(\frac{V}{150 \text{ km s}^{-1}}\right)^2 \times \left(\frac{A}{1.5 \times 10^{-6}}\right)^{-1} M_\odot \text{ yr}^{-1},$$

where V, R, and A are each expressed in units of appropriate value. The radius of the stars is 100 $R_\odot$ (Frogel, Persson, & Cohen 1983), and the velocity of the wind amounts to 150 km s^{-1}, as determined from the velocity extent of the long-wavelength wing. The value of [Mg/H] has been determined for three red giants in NGC 6752 to be -1.27 ± 0.10 (Gratton, Quarta, & Ortolani 1986), which corresponds to $A = 1.5 \times 10^{-6}$ for $(N_{Mg}/N_H)_\odot = 3.02 \times 10^{-5}$. For an optical depth $\tau_s \sim 1$, a mass loss on the order of 10^{-9} $M_\odot$ yr^{-1} would produce the observed profile asymmetry This value is commensurate with the rate suggested from studies of color-magnitude diagrams and stellar evolution calculations (Rood 1973), namely a mass loss of 0.2 $M_\odot$ during a time of $\approx 2 \times 10^8$ yr.

4. CONCLUSIONS

Strong chromospheric emission is present in both of the red giants A31 and A59 in the globular cluster NGC 6752, and GHRS spectra confirm the flux level of Mg II emission measured previously from *IUE* low-resolution spectra of A31 and suggest that chromospheric variations occur in A59. Asymmetric line profiles of the Mg II and Hα lines indicate that the atmospheres of both stars are expanding, and a spectroscopic signature of shock waves, namely a splitting of the Hα core, is apparent in A59. These measurements indicate that hydrodynamic phenomena are important in the region from which the emission originates.

The radial velocities of the cores of the optical lines range from -1 to -8 km s^{-1}. These values are less than the escape velocity from the stellar photosphere [$V_{esc} = 620(M_*/R_*)^{1/2}$ km s^{-1}], where M and R are in solar units. The escape velocity amounts to 55 km s^{-1} for a red giant ($M_* = 0.8$ $M_\odot$; $R_* =$ 100 $R_\odot$). Even if the optical line cores are formed in the extended chromosphere which might be 2 stellar radii above the photosphere, the stellar escape velocity is smaller by a factor of 0.6 (32 km s^{-1}), but its value would still exceed the velocities that we observe for these cores.

The escape velocity from the center of NGC 6752 has a value of $\sim$24 km s^{-1} (Madore 1980; Webbink 1981). Our targets lie away from the center of the cluster, so that the cluster escape velocity is less. For these stars, material lost from the star in a fast wind would be likely to escape from the cluster.

In contrast with the optical lines, the Mg II line profiles indicate outward flowing material and could show the presence of velocities substantially higher than the cluster escape velocity. Because the lines are anomalously asymmetric, it seems likely that the asymmetry results in part from an expanding wind in the red giant star. The rate of mass loss, estimated at $\approx 10^{-9}$ $M_\odot$ yr^{-1}, agrees with theoretical expectations. However, the present uncertainty in the interstellar Mg II absorption profile leaves the wind terminal velocity unknown until an interstellar line profile can be obtained. The optimum way to define the absorption profile is by observing the interstellar spectrum of Mg II against a hot continuum source, such as a horizontal branch star in NGC 6752.

We are grateful to several people at the STScI who helped to make these observations possible: Lauretta Nagel who was our official "angel" (Technical Assistant); Vicki Laidler who scanned the astrometric plates which provided the positions of A31 and A59; Ron Gilliland who kindly helped us through the intricacies of the GHRS. Mount Stromlo Observatory allowed us to borrow from their plate collection, and Gary Da Costa lent us an astrometric plate from the Yale collection. Discussions with Dimitar Sasselov concerning line profiles, and Laura Danly, Blair Savage, and Ken Sembach about the interstellar medium were extremely helpful. Support for this work was provided in part by NASA through grant number GO-2693.01-87A from the Space Telescope Science Institute, which is operated by AURA, Inc., under NASA contract NAS 5-26555. This research has made use of the SIMBAD database, operated at CDS, Strasbourg, France.

REFERENCES

Alcaino, G. 1972, A&A, 16, 220
Barnes, T. G., Evans, D. S., & Moffett, T. J. 1978, MNRAS, 183, 285
Bates, B., Catney, M. G., & Keenan, F. P. 1990, MNRAS, 245, 238
Bates, B., Kemp, S. N., & Montgomery, A. S. 1993, A&AS, 97, 937
Cacciari, C., & Freeman, K. C. 1983, ApJ, 268, 185
Cannon, R. D. 1974, MNRAS, 167, 551
Cannon, R. D., & Stobie, R. S. 1973, MNRAS, 162, 227
Castor, J. I. 1970, MNRAS, 149, 111
Clemens, D. P. 1985, ApJ, 295, 422
Cohen, J. G. 1976, ApJ, 203, L127
Colomb, F. R., Pöppel, W. G. L., & Heiles, C. 1980, A&AS, 40, 47
Crutcher, R. M. 1982, ApJ, 254, 82
Da Costa, G. S., Armadroff, T. E., & Norris, J. E. 1992, AJ, 104, 154
Danly, L., Lockman, F. J., Meade, M. R., & Savage, B. D. 1992, ApJS, 81, 125
deBoer, K. S., Lenhart, H., van der Hucht, K. A., Kamperman, T. M., Kondo, Y., & Bruhweiler, F. C. 1986, A&A, 157, 119
Duncan, D. K. 1992, GHRS Instrument Handbook, Version 3.0 (Baltimore: STScI)
Dupree, A. K., Harper, G. M., Hartmann, L., Jordan, C., Rodgers, A. W., & Smith, G. H. 1990a, ApJ, 361, L9
Dupree, A. K., Hartmann, L., & Avrett, E. H. 1984, ApJ, 281, L37
Dupree, A. K., Hartmann, L., & Smith, G. H. 1990b, ApJ, 353, 623
Dupree, A. K., Sasselov, D. D., & Lester, J. B. 1992, ApJ, 387, L85
Faulkner, D. J., & Smith, G. H. 1991, ApJ, 380, 441
Frogel, J. A., & Elias, J. H. 1988, ApJ, 324, 823
Frogel, J. A., Persson, S. E., & Cohen, J. G. 1981, ApJ, 246, 842
———. 1983, ApJS, 53, 713
Gratton, R. G., Quarta, M. L., & Ortolani, S. 1986, A&A, 169, 208
Harris, W. E., & Racine, R. 1979, ARA&A, 17, 241
Iben, I. 1991, ApJS, 76, 55
Iben, I., & Renzini, A. 1983, ARA&A, 21, 271
Johnson, H. L. 1966, ARA&A, 4, 193
Karp, A. 1975, ApJ, 201, 641
Madore, B. F. 1980, in Globular Clusters, ed. D. Hanes & B. Madore (New York: Cambridge Univ. Press), 21
Mihalas, D., & Binney, J. 1981, Galactic Astronomy (2d ed.; San Francisco: Freeman), 400
Molaro, P., Vladilo, G., & Beckman, J. E. 1986, A&A, 161, 339
Pasquini, L., Fleming, T., Spite, F., & Spite, M. 1991, A&A, 249, L23
Peterson, R. 1981, ApJ, 248, L31
Peterson, R. C. 1982, ApJ, 258, 499
Pilachowski, C. A., Sneden, C., & Wallerstein, G. 1983, ApJS, 52, 241
Roberts, M. S. 1988, in IAU Symp. 126, Harlow Shapley Symposium on Globular Cluster Systems in Galaxies, ed. J. E. Grindlay & A. G. Davis Philip (Boston: Kluwer), 411
Rodgers, A. W., & Bell, R. A. 1968, MNRAS, 138, 23
Rodgers, A. W., Van Harmelen, J., King, D., Conroy, P., & Harding, P. 1988, PASP, 100, 841
Rood, R. T. 1973, ApJ, 184, 815
Sasselov, D. D. 1993, in Nonlinear Phenomena in Stellar Variability, ed. M. Takeuti & J. R. Buchler (Boston: Kluwer), in press
Seaton, M. J. 1979, MNRAS, 187, 73P
Sembach, K. R. 1993, private communication
Sembach, K. R., Savage, B. D., & Massa, D. 1991, ApJ, 372, 81
Simon, T. 1990, ApJ, 359, L51
———. 1992, in Seventh Cambridge Workshop on Cool Stars, Stellar Systems, and the Sun, ed. M. S. Giampapa & J. A. Bookbinder (ASP Conf. Series 26), 3
Simon, T., & Drake, S. A. 1989, ApJ, 346, 303
Simon, T., Herbig, G. H., & Boesgaard, A. M. 1985, ApJ, 293, 551
Skumanich, A. 1972, ApJ, 171, 565
Smith, G. H., & Dupree, A. K. 1988, AJ, 95, 1547
Smith, G. H., Dupree, A. K., & Churchill, C. W. 1992, AJ, 104, 2005
Smith, G. H., Wood, P. R., Faulkner, D. J., & Wright, A. E. 1990, ApJ, 353, 168
Soderblom, D. R. 1993, Goddard High Resolution Spectrograph (GHRS) Instrument Handbook, Version 4.0, 43 (Baltimore: StScI)
VandenBerg, D. A. 1988, in IAU Symp. 126, Harlow Shapley Symposium on Globular Cluster Systems in Galaxies, ed. J. E. Grindlay & A. G. Davis Philip (Boston: Kluwer), 107
Wallerstein, G. 1972, PASP, 84, 656
———. 1983, PASP, 95, 422
Wallerstein, G., Jacobsen, T. S., Cottrell, P. L., Clark, M., & Albrow, M. 1992, MNRAS, 259, 474
Wakker, B. P., & van Woerden, H. 1991, A&A, 250, 509
Webbink, R. F. 1981, ApJS, 45, 259
Weiler, E. J., & Oegerle, W. R. 1979, ApJS, 39, 537
Zinn, R. 1980, ApJS, 42, 19